A high brightness source of entangled photons

Leo Wallin Sonesson

Spring of 2010

Supervisors:
o. Univ.-Prof. Dr. Anton Zeilinger
Institute for Quantum Optics and Quantum Information
Austrian Academy of Sciences
Boltzmanngasse 3, A-1090 Vienna, Austria
Leif Lönnblad
Department of Theoretical Physics
Slvegatan 14A, S-223 62 Lund, Sweden

Abstract

In the field of quantum optics and its wide variety of applications it is essential to have high brightness sources of entangled photons. In this Bachelor project, the aim has been to produce such a source based on recent experimental setups [1] [2] with a so-called Sagnac interferometer to generate polarization-entangled photons. The source built shows high quality entanglement. High visibility polarisation coincidence fringes (99.5% visibility) were observed. Moreover a Bell's inequality [6] in a CHSH-form[36] was violated by more than 44 standard deviations. Also the wavelength tuning of the source with respect to temperature and pump wavelength was analysed, revealing shifts in the degeneracy temperature of 0.020 nm/K and a shift of the signal and idler wavelengths of 0.046 nm/K.

This thesis begins with an introduction which reviews the fundamental ideas of entanglement and it's role in quantum mechanics in section 1. This section is continued by a general discussion of photonic entanglement, different types of photonic entanglement and a short discussion of how to measure this entanglement is presented. This is followed by a review of different tecniques of generating entangled photons in sections 2 and 3.

In section 4, the experimental process of assembling the Sagnac interferometer is presented. This is followed by a review of experimental results, which includes a characterisation of the source in relation to temperature and pump wavelength tunability in section 5. Then, in section **??**, a presentation and an experimental test of Bell's inequalities are presented. Thereafter, concluding remarks are made regarding the outcome of this project and the potential of further investigations utilizing the source in sections 7 and 8.

Contents

1 Introduction

Through the past century, based on very basic assumptions, modern physics have made several counterintuitive findings. To question these conclusions we must experimentally test the various hypthesis made. One of the fields that really has questioned our perceptions and preconceptions of nature is quantum mechanics. As Roger Penrose [4] remarked it "makes absolutely no sense".

Quantum mechanics raises many different issues, and one of the most perplexing and also most thouroughly studied is the result of entanglement, a concept first brought to debate by the article of Einstein, Podolsky and Rosen [3]. The term entanglement refers to several particles whose state cannot be factored into single-particle states for each particle. As such one may, for example, find that a pair of entangled photons can show strong correlations in one observable, whilst each photon independently exhibit in principle random values of this observable. The standard "Copenhagen" interpretation of quantum measurement suggests that these correlations are due to the measuring process being non-local, that is, a measurement on one particle instantly collapses the state of all particles, even if separated by a spacelike distance.

To this concept of "action at a distance", alternative theories, which do not include the idea of "non-local action", have been examined, and has led to a wide field of research. The first formulation of an experimental test wes proposed by J.S. Bell in 1964 [6]. Called Bell's inequality, it predicts that an upper limit set by classical theory is exceeded by a quantum mechanical description. Experimental tests have since been carried through, and have repetedly been found in agreement with predictions from quantum mechanics, and in disagreement with classes of local theories. Recent advances in optical technology has also made these experiments more accessible, and thereby been more reliably tested. As a part in this development, the aim of the project has focused on the methods of generating such inseperable states of photons, which will be discussed further on.

1.1 History

1933: As to the findings of quantum mechanics and it's radical consequenses, Einstein expressed a comment after a talk by Bohr in 1933, introducing a Gedankenexperiment to question the uncertainty principle on topic. Rosenfeld has recounted the argument as follows:

> "Suppose two particles are set in motion towards each other with the same, very large, momentum, and that they interact with each other for a very short time when they pass at known positions. Consider now an observer who gets hold of one of the particles, far away from the region of interaction, and measures its momentum; then, from the conditions of the experiment, he will obviously be able to deduce the momentum of the other particle. If, however, he chooses to measure the position of the first particle, he will be able to tell where the other particle is. This is a perfectly correct and straightforward deduction from the principles of quantum mechanics; but is it not very paradoxical? How can the final state of the second particle be influenced by a measurement performed on the first, after all physical interaction has ceased between them?"[5]

1935: Einstein, Podolsky and Rosen published a paper arguing that quantum theory cannot be considered complete. Again in the words of Rosenfeld the aim of the article was

> "to expose an essential imperfection of quantum theory. Any attribute of a physical system that can be accurately determined without disturbing the system, thus went the argument, is an 'element of physical reality,' and a description of the system can

> only be regarded as complete if it embodies all the elements of reality which can be attached to it. Now, the example of the two particles shows that the position and the momentum of a given particle can be obtained by appropriate measurements performed on another particle without disturbing the first, and are therefore elements of reality in the sense indicated. Because quantum theory does not allow both to enter into the description of the state of the particle, such a description is incomplete."[5]

Thus they state that there is a contradiction between classical worldview and predictions of quantum mechanics.

1965: J.S. Bell formulates a mathematical prediction which discriminates between local realistic theories and quantum mechanical predictions [6]

1972: S. Freedman and J. Clauser perform the first experimental test showing that Bell's inequality is violated [8]

1982: A. Aspect et al. perform an experiment where the analyzers are varied during the process of the test [9].

1988: Z.Y. Ou and L. Mandel [10] and (independently) Y. Shih and C.O. Alley [11] carry out the first experiment using sources with parametric down.conversion

1989: J.D. Franson [22] formulated a scheme for testing energy-time entanglement.

1990: Rarity et al. [12] realize momentum entanglement.

1992: Brendel et al. [13] were able to produce energy-time-entanglement.

1993: Kiess et al. achieve the first type-II down-conversion source for polarization-entangled photons [14]

1997: Tittel et al. [15] produce preserved correlations over distances larger than 10 km.

1999: Kwiat et al. [17] develop a different scheme made out of two type-I crystals for polarization entangled photons which achieves higher brightness.

1999: Burlakov et al [18] sets up the first entangled source based on interferometric principles.

2004-2008: Shi et al [20] set up the first Sagnac source, which is improved in recent work by Kim et al. [1] and Fedrizzi et al. [2]

1.2 Photonic entanglement

Entanglement is a quantum mechanical effect. Look at the Hilbert space $\mathcal{H}$. For a composite quantum system we can identify $\mathfrak{n}$ subsystem spaces $\mathcal{H}_i$ by the tensor product of these sybsystems:

$$\mathcal{H} = \otimes_{i=1}^{\mathfrak{n}} \mathcal{H}_i$$

Due to the superposition principle we can write any subsystem state $\mid \psi_i \rangle$ as a linear sum of its orthonormal basis vectors $\mid \psi_i \rangle = \sum_j c_j \mid k_j \rangle$ with the complex coefficients c_j. The total state of the system becomes:

$$\mid \psi_i \rangle = \sum_{j_1, j_2, \ldots, j_n} c_{j_1, j_2, \ldots, j_n} \mid k_{j_1} \rangle \otimes \mid k_{j_2} \rangle \otimes \ldots \otimes \mid k_{j_n} \rangle$$

One cannot presuppose this state to be separable, $\mid \psi \rangle \neq \mid \psi_1 \rangle \otimes \mid \psi_2 \rangle \otimes \ldots \otimes \mid \psi_n \rangle$. In the simplest generalization, we can look at two-dimensional subsystems, each seperable from each other, in four-dimensional Hilbert space. There we obtain the basis states to be the so called *Bell*, or *EPR* states:

$$\mid \psi^{\pm} \rangle = \frac{1}{\sqrt{2}} \left(\mid 0 \rangle_1 \mid 1 \rangle_2 \pm \mid 1 \rangle_1 \mid 0 \rangle_2 \right)$$

$$\mid \phi^{\pm} \rangle = \frac{1}{\sqrt{2}} \left(\mid 0 \rangle_1 \mid 0 \rangle_2 \pm \mid 1 \rangle_1 \mid 1 \rangle_2 \right)$$

or generally:

$$|\psi\rangle = \frac{1}{\sqrt{2}}\left(|0\rangle_1 |1\rangle_2 + e^{i\phi} |1\rangle_1 |0\rangle_2\right)$$

where ϕ is a arbitrary phase difference.

1.3 Different forms of entanglement

Entanglement can be actualized with many different ways. For photons, we can look at their momentum, energy, orbital angular momentum and polarization.

1.3.1 Momentum

Rarity and Tapster realized momentum entanglement in 1990. A schematic is shown in figure [12]. Two pairs of spatial (momentum, direcion) modes are chosen by pinholes from a source of entangled photons. The photons are emitted in such a way that when one photon is emitted into one of the inner two modes, its partner will be in the opposite of the outer modes due to properties of the source. The superposition of two inner and two outer modes is created by two beamsplitters, rendering the two outer and two inner indistinguishable and interference effects will appear. The state can be described as

$$\frac{1}{\sqrt{2}}\left(|U\rangle_O |L\rangle_O + e^{i\phi} |U\rangle_I |L\rangle_I\right)$$

where U signifies the upper, L the lower, O the outer and I the inner mode.

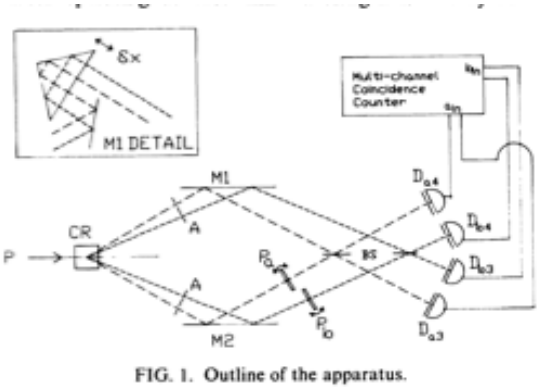

FIG. 1. Outline of the apparatus.

Figure 1: Schematic from the original paper [12]

1.3.2 Energy-Time

1989 Franson [22] proposed another type of entanglement. Photon pairs are created simultaneously by a source in the center. When there is no knowledge of the emission time a coincidence detection can detected in two indistinguishable processes. Either both photons travel along the short arm of the Mach-Zender interferometer (the straight path) och both travel the longer distance. As long as there is no knowledge of when the photons were released, entanglement will

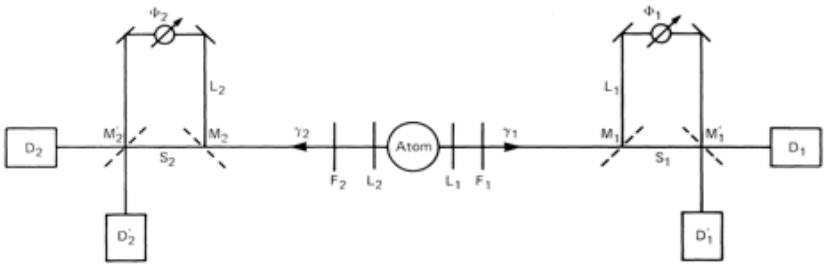

Figure 2: Schematic from the original paper [22]

occur. This can be achieved for example by utilizing an excited atom, where it's highest excited state has a relatively long lifetime, and the intermediate state has a much shorter lifetime. Then, once decay happens, it is not possible to know from which state the photon is detected.

This can be described as a state

$$\frac{1}{\sqrt{2}}\left(|\, s\rangle_1 \,|\, s\rangle_2 + e^{i(\phi_1+\phi_2)} \,|\, l\rangle_1 \,|\, l\rangle_2\right)$$

Experiments by Brendel et al. [13] and Kwiat et al. in 1992 confirmed that this type of entanglement is indeed experimentally possible.

1.3.3 Polarization

This is the most common type of entanglement, due to it's versatility to work with, and is what has been utilized in this project. From now on we will only be discussing this type of polarization, which is given by the orthogonal polarization components:

$$|\, \psi^{\pm}\rangle = \frac{1}{\sqrt{2}}\left(|\, H\rangle_1 \,|\, V\rangle_2 \pm |\, V\rangle_1 \,|\, H\rangle_2\right)$$
$$|\, \phi^{\pm}\rangle = \frac{1}{\sqrt{2}}\left(|\, H\rangle_1 \,|\, H\rangle_2 \pm |\, V\rangle_1 \,|\, V\rangle_2\right)$$

Later several methods for generating polarisation entanglement by so-called SPDC-schemes will be mentioned.

1.4 Measuring entanglement

It is important for the utilization of entangled sources to characterize a measure of entanglement in a given system. There are many common techniques to quantify entanglement, not all interchangeable. In this text two basic principles will be presented briefly. A more thourough presentation of this topic can be found in [23].

1.4.1 Coincidence fringe visibility

This is a method to test the correspondence of an given experimental state with a presumed state. The so-called coincidence fringes are calculated via joint polarization measurements on the photon pairs. Place one polarizer A to fixed at an angle α in front of one detector and another polarizer B, which has a rotational freedom of $\beta \in [0, 2\pi]$ in front of the other detector. By measuring

the number of coincident events $N(\alpha, \beta)$ at different angles, one will detect sinusoidal fringes characterized by $N(\alpha, \beta) = V \cdot \sin^2(\alpha - \beta)$, where V is the visibility $V = (N_{max} - N_{min})/(N_{max} + N_{min})$ where $N_{max} = N_{max}(\alpha, \beta)$ is the maximum number of observed coincidences, and $N_{min} = N_{min}(\alpha, \beta)$ the minimum.

With visibilities above 50% one can conclude (by measurements in a conjugate basis) that a quantum mechanical description of the electromagnetical fields of the photon pairs eliminates a classical description of the photon pairs, and with $V > 1/\sqrt{2}$ one can violate a Bell's inequality [24],[25], [26], [27].

The fringe measurement is a good charecterization of a source, but it cannot in itself generally answer if a quantum state is entangled or not, since V can reach unity for product states measured in their computational basis. Therefore one has to measure V in two conjugate bases, for example $(\alpha = 0, \alpha' = \pi/4)$.

1.4.2 Bell's inequality

Violating a Bell inequality [6] is a good way of confirming an entangled state. It gives a conclusive answer as to whether one has achieved an entangled state or not. Since a Bell's inequality was tested in this project, a more thourough explanation of the inequality is given in section 6.

2 Generating entanglement

The most common technique for generating polarization-entangled photons is in the process of spontaneous parametric downconversion (SPDC). This is a process in which a laserbeam is sent through a nonlinear medium, which usually is a custom-grown nonlinear crystal, where SPDC occurs. In this process one incoming photon (usually referred to as a pump photon) is converted into two photons (usually referred to as signal and idler photons), obeying appropriate conservation laws.

2.1 Electromagnetic waves in a medium

From electromagnetism we define polarization density to be the vector field representing the density of all electric dipole moments in a dielectric material. As such, the polarization vector $\mathcal{P}$ is per definition the dipole moment per unit volume.

A dielectric medium insulator which is effected by the action of an applied electric field thereby acquires a polarization. Placing a dielectric medium in an electric field does not make electric charges flow through the material, as in a conductor. It does however slightly shift their average equilibrium positions within the material causing dielectric polarization.

For a linear, dielectric medium is charecterized by a relation

$$\mathcal{P} = \epsilon_0 \chi \mathcal{E}$$

where ϵ_0 is the permittivity of free space and χ is the electric susceptibility of the medium. In contrast, a nonlinear, dielectric medium does not obey such a simple relation between $\mathcal{P}$ and $\mathcal{E}$.

The nonlinearity has many different forms. It may arise from either microscopic och macroscopic reasons. The density $\mathcal{P} = N$ consists of the individual dipole moment induced by the applied electric field and the number density of dipole moments N, either of which may be responsible for nonlinearities.

In most cases, the relation bewteen and $\mathcal{E}$ is linear whilst $\mathcal{E}$ is small, and nonlinearities arise when $\mathcal{E}$ comes to the same order as interatomic electric fields. To explain this we may in many cases apply a Lorentz model. If the relation between the electric field and the displacement of a charged mass can be modelled simply, following Hooke's law, that the restraining elastic force proportional to the displacement, then the polarization will be proprotional to the charge and the medium is linear. However, when this simple relation does not hold, nonlinearities start to play a role in describing the medium.

Externally applied optical electric fields are typically weak compared to charecteristic interatomic fields, and the nonlinearity is therefore usually weak. Under these circumstances, P can be expanded in a Taylorseries about $\mathcal{E}$=0

$$\mathcal{P} = \mathcal{E} + \frac{1}{2}a_2\mathcal{E}^2 + \frac{1}{6}a_3\mathcal{E}^3 + ...)$$

The coefficients are the derivatives of $\mathcal{P}$ with respect to $\mathcal{E}$, and are characteristic constants of the medium. This is often written in the form:

$$\mathcal{P} = \epsilon_0(\chi^{(1)}\mathcal{E} + \chi^{(2)}\mathcal{E}^2 + \chi^{(3)}\mathcal{E}^3 + ...)$$

where χ are the succeptibility of the material in different orders.

2.2 Second harmonic generation

For considering spontaneous downconversion of photons, it is sufficient to work to the second order. This can be described by a process called *second harmonic generation*, where we see from the above fromula that if we assume a wave of $\mathcal{E}(t) = \mathrm{Re}[E(\omega)\exp(i\omega t)]$, the second order term will have a angular frequency of 2ω (from $\mathcal{E}^2 \propto \cos 2\omega$). This term will lead to dipole radiation with an angular frequency of 2ω.

For a more general case, when we have several waves, we get *parametric interaction* of two optical waves of angular frequency ω_1 and ω_2, producing a third wave at frequency $\omega_3 = \omega_1 + \omega_2$. This is called upconversion. Similarly, the process is viable in the other direction, generating two waves out of one, which is termed downconversion.

If we look at it from quantum mechanics, we can model this process of parametric interaction as a three-photon interaction. The downconversion metioned above still has to obey all the relevant conservation rules, so we obtain the conditions:

$$\omega_p = \omega_s + \omega_i$$
$$\vec{k}_p = \vec{k}_s + \vec{k}_i$$

where the interaction described is that of the original photon, usually named the pump photon, turns into two photons, usually called signal and idler photons.

2.3 Phasematching

The interaction is highly sensitive to phase-differences along the propagation direction. A common phase-matching technique in nonlinear crystals is so called birefringent phase-matching. The properties of the non-linear medium is made in such a way that it cancels out the dispersion of the different wavelengths of the electric fields. One distinguishes two types of phase-matching, in type-I phase-matching the pump field is orthogonally oriented to the parallell signal and idler fields, whilst in type-II phase-matching, the signal and idler are orthogonal to each other.

Recently, one has been able to grow crystals with quasi-structure, so called periodically poled crystals. Here the effective nonlinearity of the medium is inverted after certain periodical distances in the crystal by the application of an electric field during the production process. This method leads to a different conservation condition:

$$\mathbf{k}_p = \mathbf{k}_s + \mathbf{k}_i + 2\pi/\Lambda(T)$$

Where $\Lambda(T)$ is a temperaturedependent constant. This makes it possible for almost arbitrary phase-matching since the crystals can be custom made as to have appropriate constants. This means that there is practically no transversal walkoff of the signal and idler beams for a type-II downconversion process, that is that one does not travel longer in the medium than the other.

3 Review of different SPDC schemes

3.1 Different crystals

One distinguishes two basic types of crystals used in the production entangled photons. In the type-I-crystal the pump field is orthogonal to the signal field and idler field, while the signal and idler fields are parallell to each other. As an example, if the pump field is initially horizontally polarized, the scheme would be $H_p \rightarrow V_i + V_s$. In type-II-crystals, you instead get a signal field orthogonal to the idler field, which in the example would correspond to $H_p \rightarrow H_i + V_s$.

3.2 The type-II single-downconverter scheme

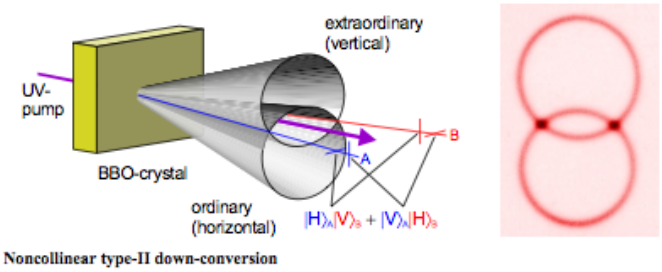

Figure 3: SPDC type II from [28]

This, the first succesful experimental configuration for production of polarization-entangled photons with this scheme was realized in 1995[16].By sending a pump-photon into a type-II crystal a signal and an idler photon can be created by spontaneous downconversion. These will have different polarization, and in a type-II crystal these two different photons propagate in different spatial directions. Due to this the photons will exit the crystal in spatially seperated directions, each in the shape of one cone due to spherical symmetries.

In most directions these two photons are perfectly distinguishable, but in the intersection of the cones, there is no knowledge from which cone, i.e. with which polarization, the photon came. Therefore, along these lines the photons will be truly entangled. They will also be spatially separated. Therefore this setup is very common and has been used in many different situations. The disadvantage of this setup is that most photons do not exit along these lines of intersection, and will thus not be entangled. Hence it is difficult to reach a high efficiency with this setup.

Utilizing this scheme has proved effective in many experiments, for example the first example of dense coding experiments [29] , the first Quantum Key Distribution (QKD) experiment with entangled photons [30], the first teleportation of an unknown quantum state [31] and production of Greenberger-Horne-Zeilinger-states (GHZ-states) [32].

3.3 The type-I sandwich scheme

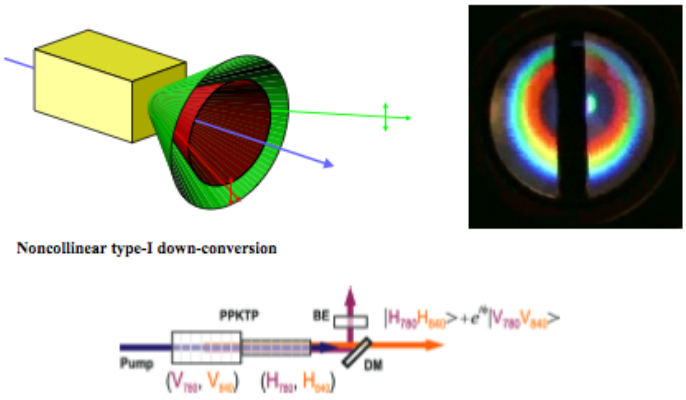

Figure 4: SPDC type II from [28], and the sandwich scheme in a schematic from [2]

Another scheme was actualized in 1999[17]. If one instead uses the other kind of crystals, the type-I crystals, arranging two crystals after each other, the second one rotated 90 degrees in respect to the first one, entanglement is produced. Here, a diagonally polarized pump photon can produce two different outcomes. Firstly, it creates a photon pair in the first crystal and go straight through the second crystal. These two photons are of one particular polarization. Secondly, it may go straight through the first crystal, and interact with the second crystal, thus yielding two photons of the other polarization. As long as there is no way of knowing the location or time in which a given photon pair are created, the resulting two photon states will be entangled.

In this scheme the exit directions-cones of photons will overlap, allowing a higher intersection, and thereby a higher degree of entanglement. There are different ways of separating the outgoing photons. One utilizes the property that this scheme allows for production of photons of two different wavelengths. Then either two horizontally polarized photons of different wavelengths or two vertically polarized photons with different wavelengths exit the crystal setup, and these photons can be separated by a dichroic mirror (DM), which lets one wavelength through, while the other is reflected.

However, to make this technique effective, one must use complex phase-matching techniques, adn it is currenly not an as popular scheme as previous one.

3.4 Inferometers: Mach-Zender

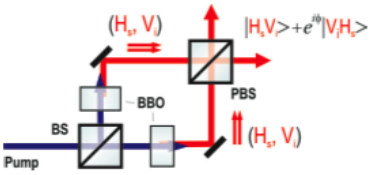

Figure 5: Schematic of Mach Zender Interferometer from [2]

Entanglement can also be achieved by placing one crystal in each arm of an inferometer and utilizing a polarizing beam splitter (see figure 5). This third type of experimental setups, utilizing a modified Mach Zender interferometer (MZI), was first introduced in 1994 by Kwiat et al. [33]. Burkalov et al. [34] were the first to report an experimental setup utilizing an interferometer in 1999, which was followed by a setup similar to that proposed by Kwiat et al. two years later by Kim et al. [35]. This scheme was later improved by Fiorentino et al. [21] who built a folded MZI, reducing phase drifts due to mechanical vibrations.

One configuration of this scheme would be as follows: the pump beam is sent through a 50/50 beamsplitter (BS), which separates the beam into two spatially separated, but otherwise identical beams. Thus for a single photon it is not known per se which arm it is in. These beams are then each sent through a type-II crystal, creating a H-V pair of photons. These pairs are sent through different sides of a polarizing beamsplitter (PBS). A PBS lets through horizontally polarized photons, while reflecting the vertically polarized photons with 90 degrees.

If we were to follow a photon through the configuration, the two possibilities would be as follows:

- The photon is goes straight through the initial beamsplitter (the chance of this happening is 50 % due to the 50/50 BS). The photon is spontaneously downconverted into a horizontally polarized and a vertically polarized photon. These enter into the polarizing beamsplitter, in which the horizontally polarized photon goes straight through, while the vertically polarized photon is reflected 90 degrees.

- The photon is reflected in the initial beamsplitter. It is then spontaneously downconverted into an H-V pair of photons, as before. But this time it enters the polarizing beamsplitter at a 90 degrees angle compared to before. Therefore the horizontally polarized photon, that exits straight through the crystal, leaves the crystal at the same angle as the vertically polarized photon of the previous possibility does. In the same manner the vertically polarized photon exits in the same direction of the polarizing beamsplitter as the horizontally polarized photon of the previous possibility.

It is therefore not possible to predict whether a single photon in one of the beams is horizontally or vertically polarized; it is an entangled photon.

There are several different setups of the Mach-Zender type. However with all of the setups it is difficult to achieve high degrees of entanglement, since mechanical vibrations creates phasedrifts in the setup. This has been tackled by some experiments, one of which was mentioned above, in these cases by actively stabilizing the interferometer.

3.5 Inferometers: Sagnac Interferometer

Another, more stable, interferometer scheme was first introduced by Shi et al [20], and improved in recent work by Kim et al. [1] and Fedrizzi et al. [2]. The starting point of a so-called Sagnac Interferometer is to send the beam through a beamsplitter, that splits the incoming beams into two overlapping beams, that go in opposite directions, and are reflected back into the beamsplitter (Figure 6a) . By using this kind of setup the beampaths are identical, and thus are not sensitive to the mechanical vibrations of the previous setup, except for rotational displacements.

To make this setup useful for applications in quantum optics we can change the beamsplitter into an dual-wavelength polarizing beamsplitter (dPBS) and add a type-II crystal in the middle of the beampath (Figure 6b). By doing this the beam that enters the clockwise path is polarized vertically polarized, while the beam entering the anti-clockwise path will be horizontally polarized. This is the basic premise for a interferometric scheme; placing non-linear crystal(s) inside separated beampaths, so that one cannot determine in which of these paths the downconversion happens, and then recombining the downconverted beams.

The type-II crystal in the middle of the beampath is meant to spontaneously downconvert the pump photon that enters in both directions. However, a type-II crystal only downconverts the photons that enter in one polarization direction. As in the type-I sandwich scheme, light of the other polarizationdirection passes straight through the crystal. One of the directions will create a signal and an idler photon, but the other direction only the pump photon will exit. To this end, we add a dual-wavelength halfwaveplate (dHWP) to our setup, changing the polarization of the pump photon entering the SI in the clockwise direction from V to H (See Figure 6 c). We also add a dichroic mirror (DM) in the output mode where the downconverted photons propagate anti-parallell to the pump photon, which reflects the photons in the downconverted photon's wavelength, while the pump photon passes straight through.

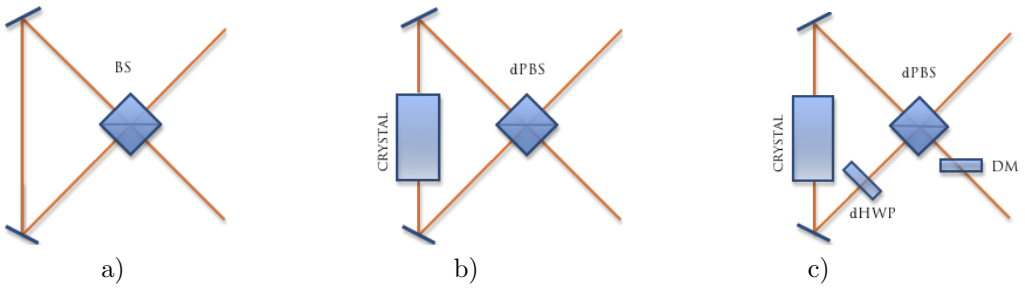

Figure 6: Schematic representation of the Polarization Sagnac Interferometer scheme with different components added. In a) the PSI is represented, in b) the PSI with a type-II downconverter crystal and in c) the PSI with a type-II downconverter and a HWP oriented at $\pi/4$ which rotates the beampolarization by $\pi/2$.

To confirm that the exiting photons are indeed entangled, let me go through the two beam-paths one by one (Figure 7):

- The counter-clockwise path:
  - A horizontally polarized photon passes straight through the DM and the dPBS.
  - In the crystal it is spontaneously downconverted into one horizontally polarized signal photon and a vertically polarized idler photon.
  - They pass through the half-wave plate, which changes the pair into one vertically polarized signal photon and a horizontally polarized idler photon.
  - The horizontally polarized idler photon passes straight through the dPBS and can then be collected.
  - The vertically polarized signal photon is reflected in the dPBS into the original pump photon's path, is then reflected by the DM, and can then be collected.
- The clockwise path:
  - A vertically polarized photon passes through the DM and is reflected through the dPBS.
  - It passes through the dHWP, which changes it's polarisation to be horizontal.
  - In the crystal it is spontaneously downconverted into one horizontally polarized signal photon and a vertically polarized idler photon.
  - The vertically polarized idler photon is reflected in the dPBS and can then be collected.
  - The horizontally polarized signal photon passes straight through the dPBS into the original pump photon's path, is then reflected by the DM, and can then be collected.

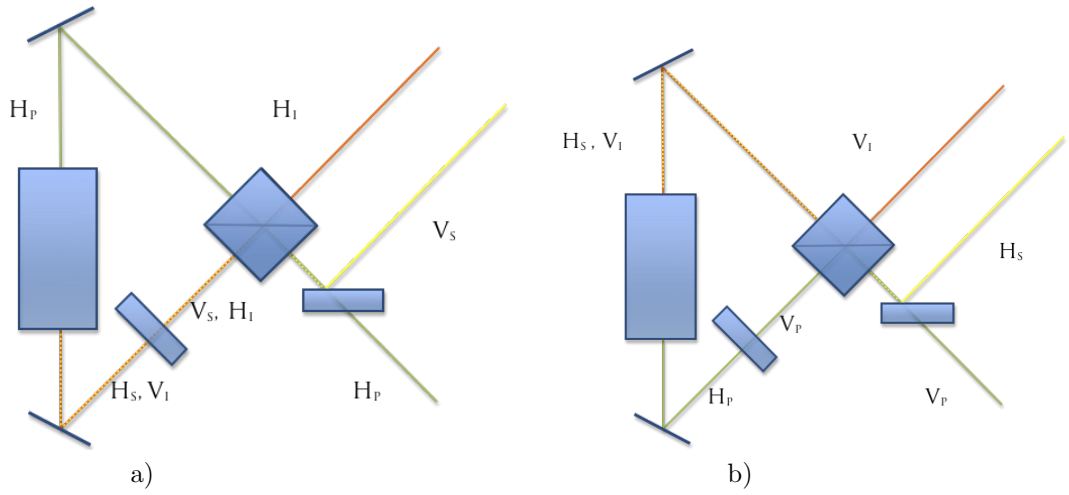

Figure 7: a) portrays the counter-clockwise path of a photon and b) portrays the clockwise path of a photon through the PSI

Therefore we see that the state emerging from the interferometer is:

$$|H_s\rangle_R |V_i\rangle_L + e^{i\phi} |V_s\rangle_R |H_i\rangle_L$$

Where R has been used to denote the right output mode in the schematic, whilst L has been used to denote the left.

The dHWP employed for the PSI is only necessary for one directions, switching the polarization state of the pumpphoton. But, as the example shows, it is very useful to have a HWP in the other direction as well.

The most simple solution, using an ordinary HWP will not work, because in the opposite direction the downconverted photons will be effected by this as if we were utilizing a quarter wave plate (QWP, assuming that $\lambda_p = \lambda_i/2 = \lambda_s/2$). Then the downconverted photons would be converted into the two circular polarization states, and would be leaving the dPBS randomly.

However, technically one could produce an instrument, which acts as a HWP on one wavelength and a full wave plate on another wavelength, leaving the downconverted photons in identical polarization states as before. But there are two reasons why it is highly beneficial to utilize the dual-wavelength HWP. The first reason has to do with the crystal. Due to birefringence in the non-linear crystal the groupvelocities of the two different polarizationstates are different. The effect of this is that the horizontally polarized signal-photon effectively leaves the crystal before the vertically polarized idler-photon. But, by utilizing a dHWP this temporal walkoff is neutralized by inversing the polarization states for one of the paths. Therefore the signal (idler) photon of one path couples to the signal (idler) photon of the other path. There will still be a delay in arrival time of the photons, but the difference no longer creates any information about the polarization state of the photons. This greatly increases the quality of entanglement in the setup. A schematic is given in figure 8.

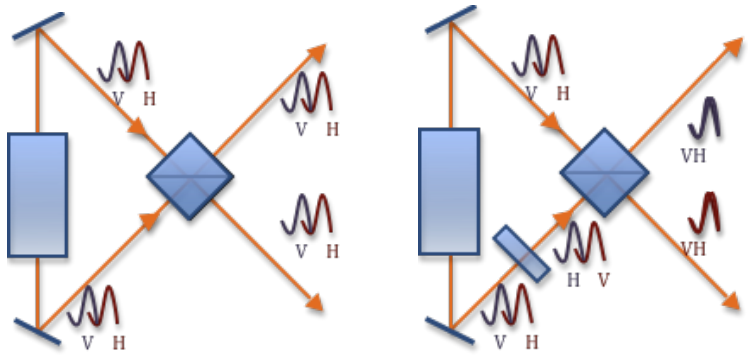

a) b)

Figure 8: Figure a) depicts the setup without a dHWP and b) how the dHWP compensates for the walkoff and couples each signal (idler) to the other possible signal (idler)

Secondly, a conceptually interesting feature emerges. Since each signal (idler) photon now couples to the signal (idler) photon the entanglement would still be present in a non-wavelength-degenerate case, $\lambda_s \neq \lambda_i$. That this walkoff compensation is wavelength-independent is so far unique to this configuration.

4 Experimental work

In the following paragraphs the process of building the source is discussed.

4.1 Laser diodes

A laser diode basically consists of three parts, a *gain medium* located inside a *cavity* (a series of mirrors set up as to repeteadly reflect light in between them, with typically one mirror transmitting some portion of light while reflecting the rest) subject to *electric pumping*. The basic idea is that an electric current excites the atoms inside the cavity. As they are relaxed, they emit light. The cavity then reflects the light back and forth, accumulating larger and larger amounts of photons. Due to interference of the reflections, only some standing wave patterns will be amplified, while other patterns will decrease due to destructive interference. As the standing waves are wavelength-dependent, this will in principle single out a few wavelength of the emitted ones, something one refers to as a *single-mode*. In practice, the laser diode exhibits several peaks of different wavelengths due to techichal factors, and therefore needs to be stabilized before use.

For the setup a 250 mA laserdiode with emmision wavelegths around 400-410 nm was employed. Measurements were made to characterize the laserdiode in terms of it's power-current dependence, and the results can be seen in figure 9.

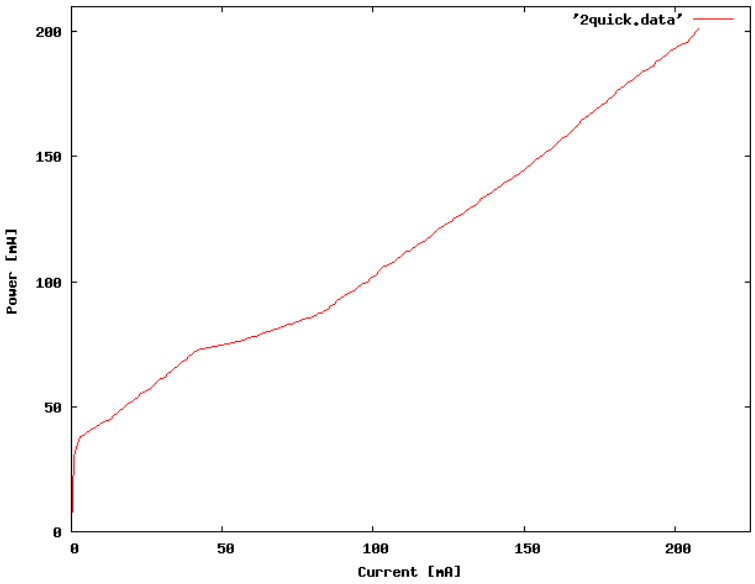

Figure 9: Characterization of laser diode

4.2 Laser Diode Testing

The components of the Sagnac setup, such as the PPKTP and the dPBS, are highly wavelength-dependent. However, a laser diode doesn't produce photons of a single wavelength. In general it exhibits several different peaks in intensity around different wavelengths, one says that it is *multimoded*.

Therefore, optimization of the laserbeam is necessary. First we tested some standard techniques were tested, whilst later some original techniques were employed. The most important aspect while *stabilizing* the beam is to make sure that it only exhibits a peak around one wavelength, that it is *singlemoded*. Other aspects that are important is that one can retrieve the largest amount of power possible after the stabilization, that the beam is not astigmatic and that the setup is easy to adjust.

All setups use the idea of optical feedback to stabilize the laser. In this idea one uses an wavelength-tunable external cavity. The most common example is called the Littrow configuration (see figure 10). In this one directs the laser towards a diffraction-grating. This will produce maximas of different orders with specific wavelengths. One of these orders are then directed back into the laser, creating an external cavity. This external cavity will then amplify the wavelength it is tuned to, effectively stabilizing the laser.

The distance between different wavelengths in the internal cavity will display maximas separated by a distance of the *free spectral range*, the frequency spacing of its resonator modes, which is given by FSR= $c/2L$. So since the distance length of the internal cavities are relatively small, the free spectral range is relatively large compared to the external cavity. However, the maximas of the external cavity are damped around the optimum wavelength. Therefore, many of the maximas of the internal cavity will be damped. However, since the free spectral range of the internal cavity is even smaller, within this region there will be even more possible wavelengths (if the length is long of a standing wave, it is 'easier' to add another mode to the standing wave, and they will lie closer). But only one mode will be amplified in the end because of modecompetition. What is meant by this is that the mode on the absolute maxima of the wavelength-selectivity will be a little bit larger than any of the other. When iterated through the cavity several times this small difference will become larger every time, and in actual laser setups it will become much larger than any other mode.

For this setup to be effective one needs an external cavity with a high wavelength-selectivity, thus minimizing the number of external cavity modes, and a small cavity size, so the spacing between different modes of the external cavity will be maximal.

After testing one of the standard techniques, the Littrow configuration (see figure 10a), the other standard setup was also tested. This is the Littman-Metcalf configuration (see figure 10b). In the Littman-Metcalf configuration one fixes the grating orientation, and employs an additional mirror to reflect the first-order beam back into the laser diode. By rotating this additional mirror one can tune the wavelength of the beam. This setup usually results in a smaller linewidth (a more narrow peak around a maximum wavelength), due to the fact that the wavelength selectivity is stronger. It is also a more flexible setup to work with, since one can tune the wavelength of the beam without moving the spatial position of the beam. The disadvantage of this setup is that the zero-order reflection of the diffraction grating is lost, so that the output power is lower than for the Littrow configuration.

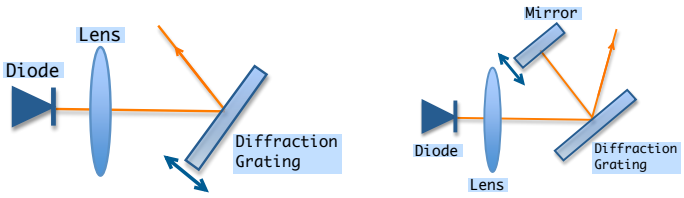

Figure 10: The Littrow and the Littman-Metcalf external cavity scheme respectively

At this point, some less common configurations involving a beamsplitter were tested to reduce loss of pump-power in the cavity. Utilized as a beamsplitter was a dielectric mirror reflecting $\frac{1}{2}$ of the incoming beam. Firstly, we tested one setup with the dielectric mirror and a diffraction-grating. Here, we reduced the intensity of the feedback by transmitting $\frac{1}{2}$ of the beam, and using a Littrow-configuration with the remaining third. With this setup we could effectively lower the feedback-pump-power ratio, and thereby achieve feedback with less loss of power. Due to our relatively high pump-power in the region of 200 mW, there was room for this adjustment, since not such a large feedback is needed.

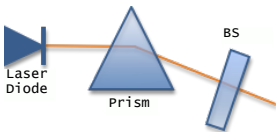

Figure 11: External cavity used in experiment

Secondly, we tried out a setup involving a prism and the dielectric mirror (see fig 11). Since the prism only has one output for each wavelength, as compared to the diffraction grating's many different orders, the setup allows us to, in principle, lose none of the pump power in the feedback process (the power of the outputs with other wavelengths than our desired one would be lost, but this would never be utilized). The wavelength could then be tuned in this configuration by rotating the dielectric mirror, thereby changing the FSR of the external cavity.

This setup ended up being the one we chose to work with, due to the easy tunability, high power and low linewidth. The resultant beam characterization, in terms of wavelength can be seen in figure 12.

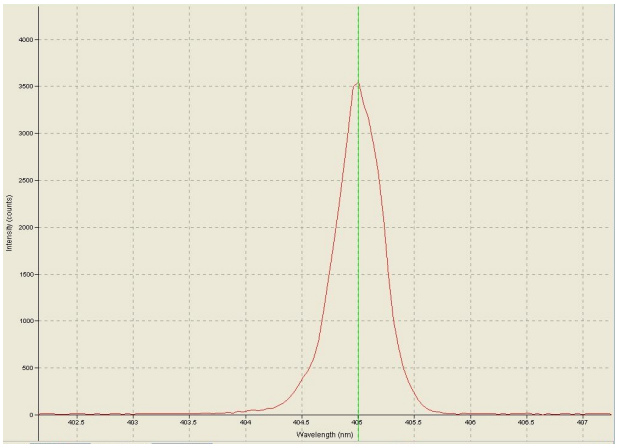

Figure 12: Intensity measured as function of wavelength after external cavity

4.3 Choice of focusing lens

The collimated beam from the external cavity was measured to have a spot of approximately 1.5mm. Previous measurements on various crystals have been used to show that an optimal spotsize in the 20 mm PPKTP crystal, which we utilized, was in the region of 70 μm. The method chosen for coupling in the singlemode fibers (with mode field diameter of 5.6 μm) into the photon detector was mounting 10x objectives (with effective focal length of 18 mm) on a high precision coupling. This, together with the desired spotsize inside the crystal (70 μm) decided the working distance to the couplers:

$$\begin{aligned} \theta_0' z_0' = W_0' = W_0 = \theta_0 \\ \Leftrightarrow \frac{z_0' \lambda}{\pi \omega_0'} = \frac{z_0 \lambda}{\pi \omega_0} \\ \Leftrightarrow \frac{z_0'}{\omega_0'} = \frac{z_0}{\omega_0} \end{aligned}$$

With z_0' to be the effective focal length, ω_0' to be the mode field diameter and crystal spot size to be ω_0, one calculates a working distance from the coupler to the crystal of $z_0 = 22.5cm$.

By this measure, we could now choose an appropriate lens for focusing the collimated beam coming from the cavity. To maximize the length of to the coupler, the PSI's size was minimized. Several mirrors and a beamsplitter needed to be fit into the path between the lens and the crystal.

For focusing the collimated beam, the approximation that the working distance is equal to the depth of focus is a good approximation. An 200mm focal length lens was calculated to produce a spotsize of approximately 69 μm, and was therefore deemed to be the most appropriate, a longer focal length would have resulted in a too large spotsize.

4.4 Setting up the Sagnac source

For the setup, a 20 mm PPKTP crystal was utilized in the PSI. The PSI also included with a dPBS, dHWP and two mirrors with high reflectivity at both involved wavelength-regions, 405 and 810 nm.

The method for aligning the source was to roughly align the PSI. Thereafter, the pump beam was sent through the PSI, with one mirror taken out. We then measured the exact working distance to the spot. Thereafter the last mirror was inserted, and the output was sent through a polarizer at 45 degrees. Therefore the two arms of the interferometer could show interference patterns. When these were maximized, the arms were roughly equal.

Thereafter the couplers were mounted and roughly aligned to the PSI with an alignment laser sending beams backwards through the setup. After this the alignment of the entire setup was finely adjusted by optimizing countrates.

4.5 Overview of the source

See figure 14. The laser diode with external cavity was coupled through singlemode fibre to the PSI. This was chosen since, even though it implied a reasonable loss in power, the properties of the beam became very well-behaved, in contrast to the initial beam, which included some issues such as astigmatism and non-homogeneity. For a charecterisation of the output beam in terms of it's intensity, as shown by a CCD image, see figure 13.

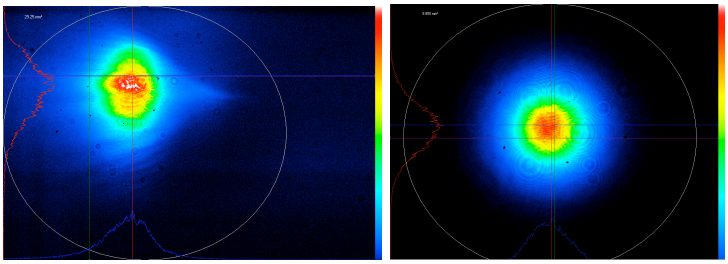

Figure 13: CCD image of the beam before respectively after going into a single mode fibre

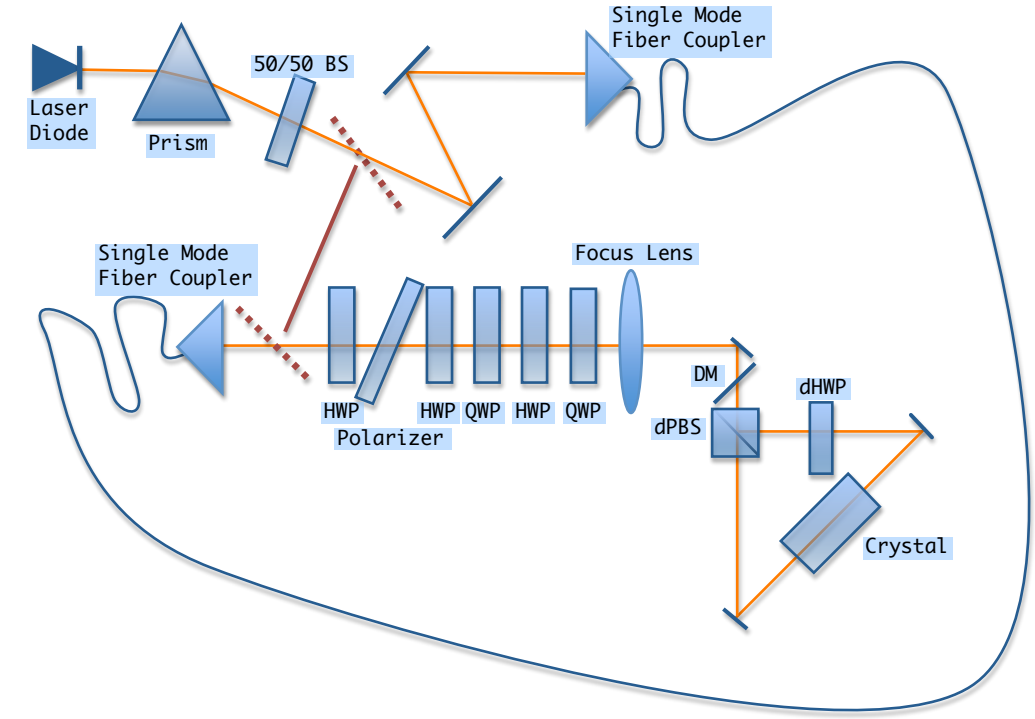

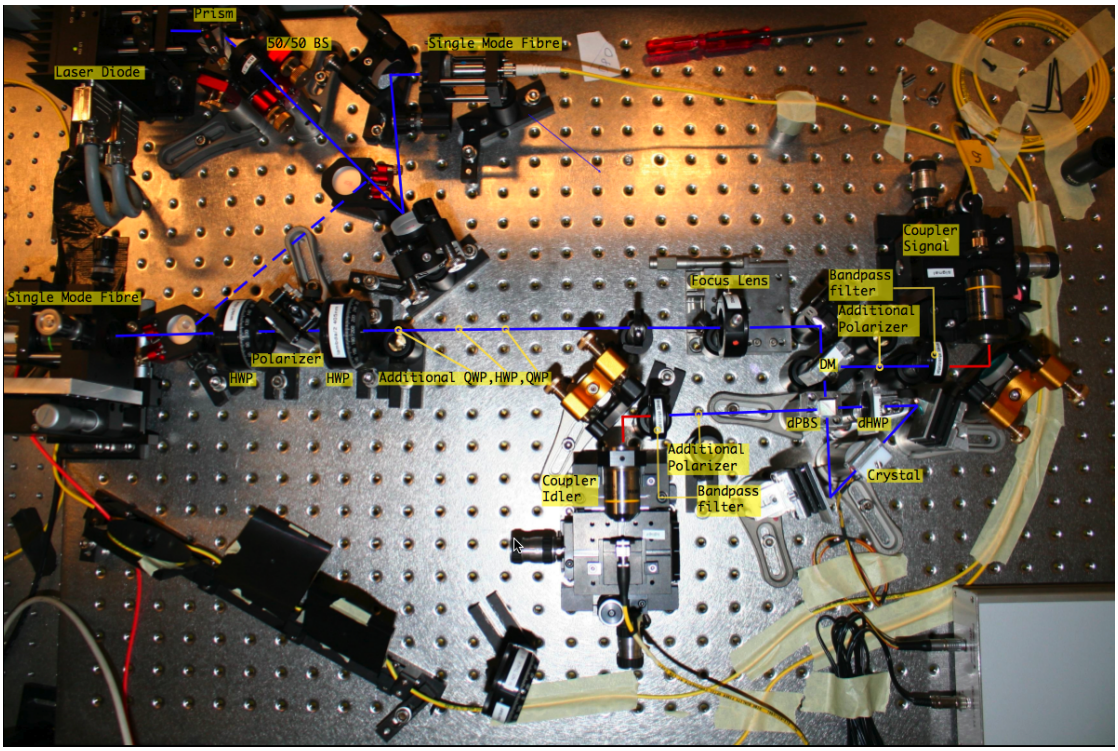

Figure 14: Schematic and picture of the experimental setup

5 Temperature and wavelength dependence

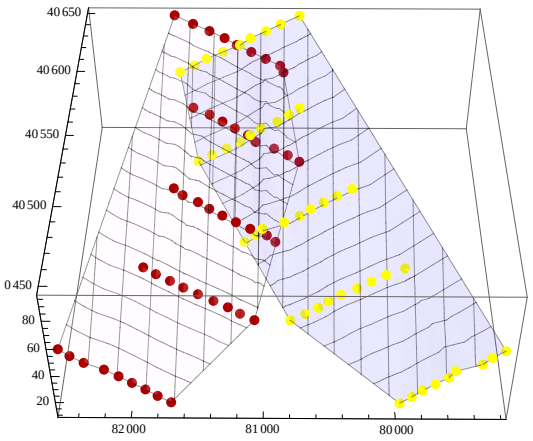

Figure 15: Charecteristics of the source in terms of temperature and pump wavelength

The setup allowed us to vary the wavelength of the pump-beam as well as the temperature of the oven containing the crystal. We therefore worked to find an optimum setup for our experiment, producing an 810-nm signal and idler photon pair at a suitable wavelength. The result is indicated in the graphs. This will be useful in allowing us to optimize the source.

For different pump wavelengths the temperature of the crystal was varied, and the resultant wavelengths of the signal and idler photons can be found in figure **??**. At each intersection we find degenerate temperature

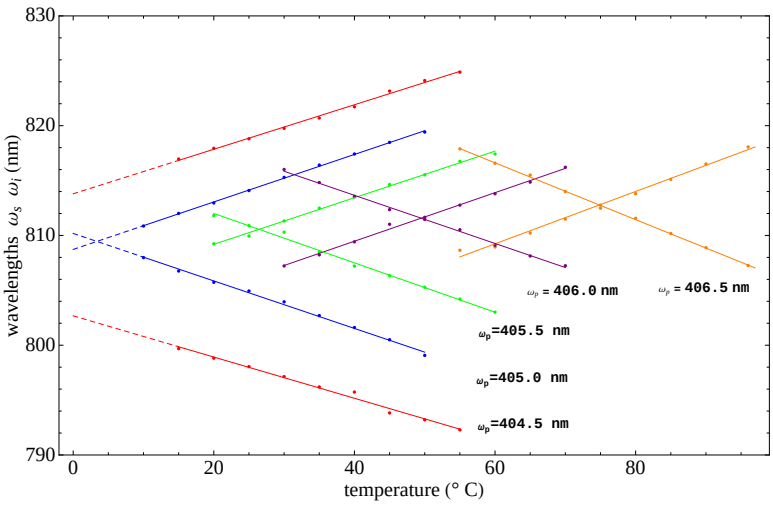

Figure 16: Wavelength of signal and idler photons dependence on temperature

The degenerate temperature was then plotted as a function of pump wavelength and signal/idler wavelength, to be used to choose a suitable working regime. We shifts in the degeneracy

temperature of 0.020 nm/K for pump wavelengths and a shift of the signal and idler wavelengths of 0.046 nm/K.This is seen in figure 17 and 18.

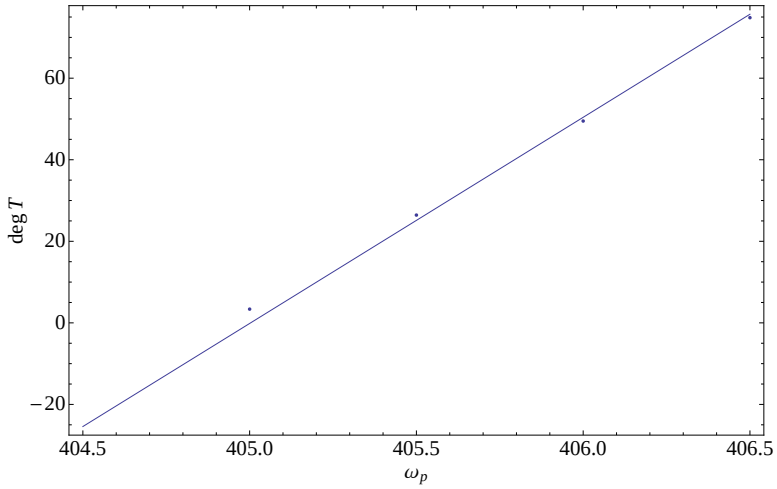

Figure 17: Degenerate temperature for different pump wavelengths

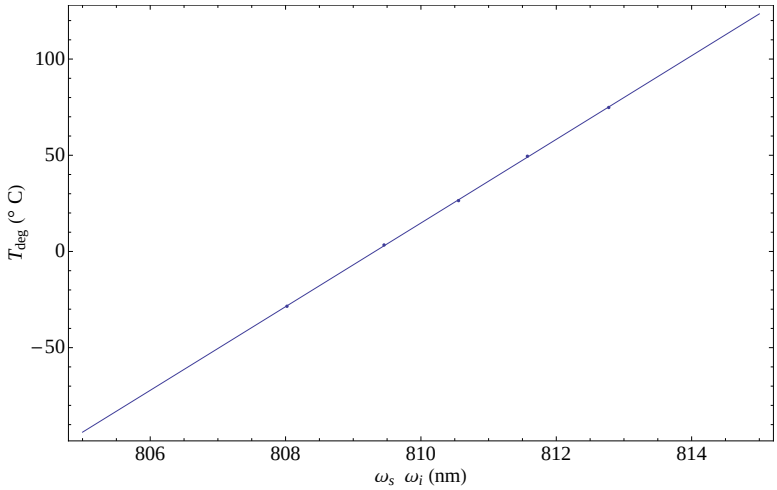

Figure 18: Degenerate temperature for different signal/idler wavelengths

6 Violating Bell's Inequality

To confirm that the source was indeed running, polarizers were placed in front of each coupler.

6.1 Introduction

We will in the following be deriving and evaluating the Bell Inequalities in the Clauser-Horne-Shimony-Holt form (CHSH) [36] [37] utilizing one of the four mixed quantum states usually referred to as the Bell states, namely that of the $|\psi^-\rangle$ state:

$$|\psi^-\rangle = |H_s\rangle|V_i\rangle - |V_i\rangle|H_s\rangle$$

An idealised schematic can be seen in figure 19.

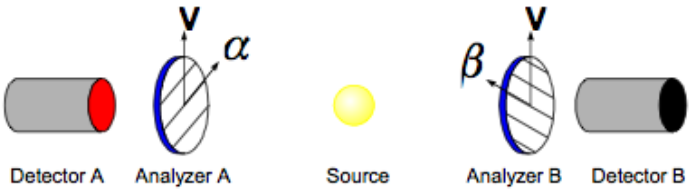

Figure 19: Schematic of an experiment that measures correlations between two systems originating from a common source

Measurement of this state can be made by projections onto different bases. Any valid bases of measurement could be characterized by it's angle from the horizontal axis α respectively β, depending on the detector in question:

$$|\alpha\rangle = \cos\alpha|H\rangle + \sin\alpha|V\rangle$$

where for example a measurement with $\alpha = 45$ degrees would correspond to measuring in a diagonal basis.

Now what is the probability of finding a photon from our original $|\psi^-\rangle$-state if we measure it in some arbitrary basis of measurement?

$$P(\alpha,\beta) = |\langle\alpha|\langle\beta||\psi^-\rangle|^2 = \frac{1}{2}(\cos\alpha\sin\beta - \sin\alpha\cos\beta)^2 = \frac{1}{2}\sin^2(\alpha-\beta)$$

One can then define the expectation value of the product of simultaneous polarization measurements to be:

$$E(\alpha,\beta) = P(\alpha,\beta) + P(\alpha_\perp,\beta_\perp) - P(\alpha_\perp,\beta) - P(\alpha,\beta_\perp)$$

where $\alpha_\perp = \alpha + 90°$ and $\beta_\perp = \beta + 90°$.

This covers all possible outcomes and it's value varies from +1 when the polarizations always agree to -1 when they always disagree. Thereby it is also to be seen as the correlation coefficient of each side.

For our state this becomes:

$$\begin{aligned} E^{\psi^-} &= \frac{1}{2}\left(\sin^2(\alpha-\beta) + \sin^2(\alpha+90°-\beta-90°) - \sin^2(\alpha+90°-\beta) - \sin^2(\alpha-\beta-90°)\right) = \\ &= \sin^2(\alpha-\beta) - \cos^2(\alpha-\beta) = -\cos[2(\alpha-\beta)] \end{aligned}$$

From this we see that the correlation does not depend on an absolute angle, but rather on the difference between the two angles of measurement. If we have a difference in angle of 90° we see that the system shows perfect correlation, E=+1, and if we measure with no difference of angle, i.e. 0°, we see perfect anticorrelation, E=-1.

6.2 Local realism

The "Copenhagen" interpretation of quantum measurements argues that these correlations arise from a nonlocality of the measurement process: a measurement on one particle instantly collapses the state of both particles, even at an arbitrary separation. The two fundamental implication of this interpretation are the following: firstly, until measurement is made, the particle is truly in a mixed state, where it is neither decidedly one of it's possible values. This is usually referred to as non-realism, since, if you are a realist you believe that that particle has a true set of values whether you measure it or not (for example you believe that the moon is still there, even though you're not looking at it). Secondly, non-locality is inferred. This is the notion that things cannot influence each other on remote distances of each other.

So let's make the two assumptions of realism and local action. Then whatever theory we were to find, it would be a function of some for us unknown parameter. Call this hidden variable $\lambda \in \Lambda$, and say that it's distribution is $\rho(\lambda)$. Expectation values are given by integrating the variables over the hidden variable space. For the two observables $A(\alpha,\lambda), B(\beta,\lambda) \in \{-1,1\}$, we get the expectation value of their product by:

$$E(\alpha,\beta) = \int_\Lambda d\lambda\ \rho(\lambda) A(\alpha,\lambda) B(\beta,\lambda)$$

We can derive an upper limit for all values possible by manipulation this expression in the following way, which is referred to as the CHSH form:

$$\begin{aligned}
&E(\alpha',\beta') + E(\alpha',\beta) = \\
&= \int_\Lambda d\lambda\ \rho(\lambda)\left[A(\alpha',\lambda)B(\beta',\lambda) + A(\alpha',\lambda)B(\beta,\lambda)\right] = \\
&= \int_\Lambda d\lambda\ \rho(\lambda)[A(\alpha',\lambda)B(\beta',\lambda) + A(\alpha',\lambda)B(\beta,\lambda) \pm \\
&\pm A(\alpha,\lambda)B(\beta,\lambda)A(\alpha',\lambda)B(\beta',\lambda) \mp A(\alpha,\lambda)B(\beta',\lambda)A(\alpha',\lambda)B(\beta,\lambda)] = \\
&= \int_\Lambda d\lambda\ \rho(\lambda)[(A(\alpha',\lambda)B(\beta',\lambda)(1 \pm A(\alpha,\lambda)B(\beta,\lambda)) \\
&+ (A(\alpha',\lambda)B(\beta,\lambda)(1 \mp A(\alpha,\lambda)B(\beta',\lambda))
\end{aligned}$$

so

$$\begin{aligned}
&|E(\alpha',\beta') + E(\alpha',\beta)| \leq \\
&\leq \int_\Lambda d\lambda\ \rho(\lambda)(1 \pm A(\alpha,\lambda)B(\beta,\lambda)) + \int_\Lambda d\lambda\ \rho(\lambda)(1 \mp A(\alpha,\lambda)B(\beta',\lambda)) = \\
&= 2 \pm |E(\alpha',\beta') - E(\alpha,\beta')|
\end{aligned}$$

Where we in the last line took the absolute values of all the independent components. From this we choose the negative sign and define the Bell parameter to be:

$$S(\alpha,\alpha',\beta,\beta') = |E(\alpha,\beta) - E(\alpha,\beta')| + |E(\alpha',\beta') + E(\alpha',\beta)| \leq 2$$

This tells us that every theory explained by a local hidden variable must obey this limit.

6.3 Violation of Bell's inequality

We can calculate this Bell parameter using the expectation values we derived in the section for quantum mechanics as well. For a certain system of angles we then see that we can actually break the inequality. For:

$$S(0°, 22.5°, 45°, 67.5°) = |-\cos 45° + \cos 135°| + |-\cos 45° - \cos 45°| = 2\sqrt{2} > 2$$

In experiments exactly this value may not be possible to achieve, because of non-ideal configurations, but one may still achieve values larger than 2 of the Bell Parameter.

6.4 Experimental Test of Bell's inequality

We have the general definition of the correlations:

$$E(\alpha, \beta) = P(\alpha, \beta) + P(\alpha_\perp, \beta_\perp) - P(\alpha_\perp, \beta) - P(\alpha, \beta_\perp)$$

Using:

$$P(\alpha, \beta) = N(\alpha, \beta)/N_{tot}$$

where N_{tot} is given by

$$N_{tot} = N(\alpha, \beta) + N(\alpha_\perp, \beta_\perp) + N(\alpha_\perp, \beta) + N(\alpha, \beta_\perp)$$

We can measure the quantity $E(\alpha, \beta)$ with four measurements:

$$E(\alpha, \beta) = \frac{N(\alpha, \beta) + N(\alpha_\perp, \beta_\perp) - N(\alpha_\perp, \beta) - N(\alpha, \beta_\perp)}{N(\alpha, \beta) + N(\alpha_\perp, \beta_\perp) + N(\alpha_\perp, \beta) + N(\alpha, \beta_\perp)}$$

And can then calculate:

$$S(\alpha, \alpha', \beta, \beta') = E(\alpha, \beta) - E(\alpha, \beta') + E(\alpha', \beta') + E(\alpha', \beta)$$

from 16 measurements. These measurements were made using the PSI. The beam sent into the PSI went through one HWP and one QWP, so that a diagonal state could be achieved. This was done and Table 1.1 shows the result. As for calculation of the standarddeviation, the distribution goes towards a gaussian distribution for large n, and therefore was evaluated by errorprogression of the square roots of the measured quantities.

We found $S = 2.499 \pm 0.0113$, a violation of Bell's inequality with over 44 standarddeviations, a result in inconsistent to explain with local hidden variable theories, and in accordance with quantum mechanical predictions.

	0	90	45	-45
22.5	5069	67719	22992	52154
112.5	26993	12429	34487	3434
67.5	26738	10965	3462	33400
-22.5	5360	66514	55384	20400

E(a,b)	E(a,b')	E(a',b)	E(a',b')
-0,576	0,533	-0,702	-0,688

S	2,499±0,0113

Table 1: Measurements violating Bell's inequality

6.5 Measurement of the coincidence fringe visibility

In conjunction with the measurements on the Bell's inequality, a good measurement characterizing the source was fitting to carry out, the fringes measurement mentioned in section 1.4.1. The result is given in figure 20. In the same series of measurements, the visibility was found to be 99.5% in H-V. These numbers are presented without accidental corrections. The deviations in the higher degrees can be explained by difficulty in mounting the polarizers responsible for the different polarizations, which was also the reason more elaborate measurements for characterizing the source were not carried out in this project.

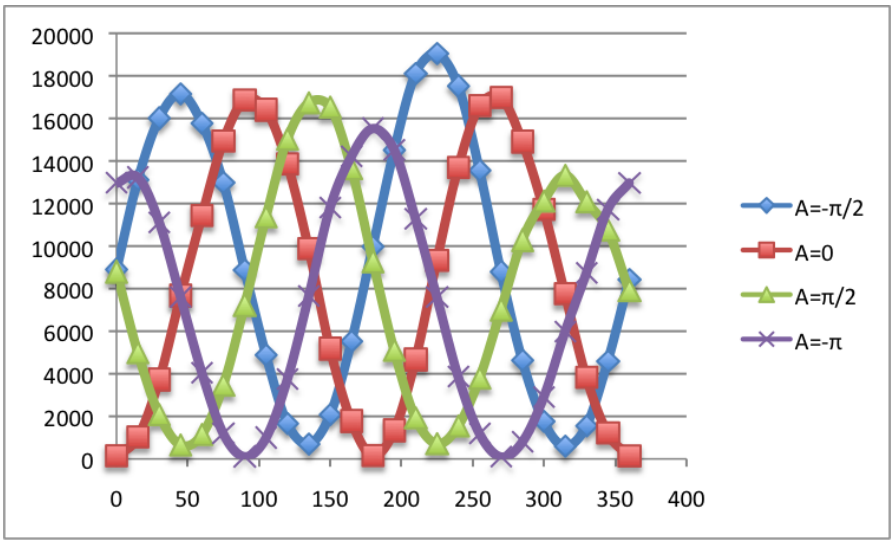

Figure 20: Coincidence fringe visibility

7 Outlook

This source shows great potential at becoming useful at higher powers. In the scope of this project, it has not been running at maximum capacity, but the potential to improve is evident. This may be useful since the source will be able to be being coupled into future experiments, leading to detectable results not only with single photon detectors, but with such devices as CCD imaging.

To illustrate this principle, with the single mode fibre we were never able to couple out more than 5 mA, whilst while working in free space we could have a maximum current of 200 mA, an increase in of a factor 40. The effect of working under these conditions were a decreased visibility, at a maximum at 97,1 %.

8 Conclusion and Acknowledgements

In conclusion, a Sagnac Interferometer was constructed, based on polarization entangled photons. In functional form, the Bell's inequalities were violated by 44 standard deviations. Also, a measurement as to suitable temperature conditions for the crystal was carried out, which will prove useful for future assemblies and calibration of sources. The source was predicted to be able to work at currents of 200 mA, which will be useful for future experiments.

I would like to acknowledge the kind support of the Institute for Quantum Optics and Quantum Information and Prof. Anton Zeilinger, where this project was carried out, together with Sven Ramelow, Marcin Wiesniak, Robert Fickler, Radoslaw Lapkiewicz and Christoph Schäff. I would also like to acknowledge the University of Lund and my local supervisor Leif Lönnblad.

References

[1] T. Kim, M. Fiorentino, and F.N.C. Wong. Phase-stable source of polarization- entangled photons using a polarization Sagnac interferometer. Physical Review A, 73(1):12316, 2006.

[2] Alessandro Fedrizzi, *Fundamental experiments with a high brightness source of entangled photons.* Betrreuer: o. Univ.-Prof. Dr. Anton Zeilinger, University of Vienna, A 091 411, 2008.

[3] A. Einstein, B. Podolsky, and N. Rosen, "Can quantum-mechanical description of physical reality be considered complete?" Phys. Rev. **47**, 777–780 (1935).

[4] Roger Penrose: Gravity and State Vector Reduction. In "Quantum Concepts in Space and Time", eds. R. Penrose and C.J. Isham, Clarendon Press, Oxford (1986) 129.

[5] L. Rosenfeld, "Niels Bohr in the thirties: consolidation and extension of the conception of complementarity," in *Niels Bohr: His life and work as seen by his friends and colleagues,* S. Rozental, ed., (North-Holland, Amsterdam, 1967).

[6] J. S. Bell, "On the Einstein-Podolski-Rosen Paradox," Physics (Long Island City, NY) **1**, 195–200 (1964). This article is reprinted in [7].

[7] J. A. Wheeler and W. H. Zurek, *Quantum Theory and Measurement* (Princeton University Press, Princeton, NJ, 1983).

[8] S. J. Freedman and J. F. Clauser, Phys. Rev. Lett. 28, 938 (1972).

[9] A. Aspect, J. Dalibard, and G. Roger, Phys. Rev. Lett. 49, 1804 (1982).

[10] Z. Y. Ou and L. Mandel, Phys. Rev. Lett. 61, 50 (1988).

[11] Y. H. Shih and C. O. Alley, Phys. Rev. Lett. 61, 2921 (1988).

[12] J. G. Rarity and P. R. Tapster, Phys. Rev. Lett. 64, 2495 (1990).

[13] J. Brendel, E. Mohler, and W. Martienssen, Europhys. Lett. 20, 575 (1992).

[14] T. Kiess, Y. Shih, A. Sergienko, and C. Alley, Phys. Rev. Lett. 71, 3893 (1993)

[15] W. Tittel, J. Brendel, H. Zbinden, and N. Gisin, Phys. Rev. Lett. 81, 3563 (1998).

[16] P. G. Kwiat, K. Mattle, H. Weinfurter, A. Zeilinger, A. V. Sergienko, and Y. Shih *New High-Intensity Source of Polarization-Entangled Photon Pairs.* Physical Review Letters, 75(24):43374341, 1995.

[17] P.G. Kwiat et al., Phys. Rev. A 60, R773 (1999).

[18] A. V. Burlakov, M. V. Chekhova, O. A. Karabutova, D. N. Klyshko, and S. P. Kulik. Polarization state of a biphoton: Quantum ternary logic. Physical Review A, 60(6):R4209R4212, Dec 1999.

[19] Y. H. Kim, M. V. Chekhova, S. P. Kulik, M. H. Rubin, and Y. Shih. Interferometric bell-state preparation using femtosecond-pulse-pumped spontaneous parametric down-conversion. Physical Review A, 63(6):062301, May 2001. 2

[20] B. S. Shi and A. Tomita. Generation of a pulsed polarization entangled photon pair using a Sagnac interferometer. Physical Review A, 69(1):13803, 2004.

[21] M. Fiorentino, G. Messin, C. E. Kuklewicz, F. N. C. Wong, and J. H. Shapiro. Gen- eration of ultrabright tunable polarization entanglement without spatial, spectral, or temporal constraints. Physical Review A, 69(4):41801, 2004

[22] J. D. Franson, Phys. Rev. Lett. 62, 2205 (1989).

[23] S. J. van Enk, N. Ltkenhaus, and H. J. Kimble. Experimental procedures for entanglement verication. Physical Review A, 75(5):52318, 2007

[24] R. Ghosh and L. Mandel. Observation of nonclassical e?ects in the interference of two photons. Physical Review Letters, 59(17):19031905, Oct 1987

[25] A. Shimony M. Horne and A. Zeilinger. Down-conversion photon pairs: A new chapter in the history of quantum mechanical entanglement. Quantum Coherence, Jeeva Anandan (Ed.), World Scientic Publishing Co., Singapore, 1990.

[26] J. D. Franson. Violations of a simple inequality for classical elds. Physical Review Letters, 67(3):290293, 1991

[27] P. G. Kwiat, A. M. Steinberg, and R. Y. Chiao. High-visibility interference in a Bell- inequality experiment for energy and time. Physical Review A, 47(4):24722475, 1993

[28] Gregor weihs, *Introduction to Photonic Entanglement.* Lecture given at Seminaire Rhodanien, 2000.

[29] K. Mattle, H. Weinfurter, P. G. Kwiat, and A. Zeilinger. *Dense coding in experimental quantum communication.* Physical Review Letters, 76(25):46564659, Jun 1996.

[30] T. Jennewein, C. Simon, G. weihs, H. Weinfurter, and A. Zeilinger. *Quantum Cryptography with Entangled Photons.* Physical Review Letters, 84(20):47294732, 2000.

[31] D. Bouwmeester, A. K. Ekert, and A. Zeilinger. *The Physics of Quantum Information: Quantum Cryptography, Quantum Teleportation, Quantum Computation.* Springer, 2001.

[32] D. Bouwmeester, J. W. Pan, M. Daniell, H. Weinfurter, and A. Zeilinger. *Observation of Three-Photon Greenberger-Horne-Zeilinger Entanglement* Physical Review Letters, 82(7):13451349, 1999. 26, 76

[33] P. G. Kwiat, P. H. Eberhard, A. M. Steinberg, and R. Y. Chiao. Proposal for a loophole-free Bell inequality experiment. Physical Review A, 49(5):32093220, 1994. 28

[34] A. V. Burlakov, M. V. Chekhova, O. A. Karabutova, D. N. Klyshko, and S. P. Kulik. Polarization state of a biphoton: Quantum ternary logic. Physical Review A, 60(6):R4209R4212, Dec 1999. 28

[35] Y. H. Kim, M. V. Chekhova, S. P. Kulik, M. H. Rubin, and Y. Shih. Interferometric bell-state preparation using femtosecond-pulse-pumped spontaneous parametric down-conversion. Physical Review A, 63(6):062301, May 2001. 28, 38

[36] J. F. Clauser, M. A. Horne, A. Shimony, and R. A. Holt. Proposed Experiment to Test Local Hidden-Variable Theories. Physical Review Letters, 23(15):880884, 1969.

[37] S. J. Freedman and J. F. Clauser. Experimental test of local hidden-variable theories. Physical Review Letters, 28(14), 1972.